PERGAMON

International Journal of Plasticity 17 (2001) 537–563

INTERNATIONAL JOURNAL OF Plasticity

www.elsevier.com/locate/ijplas

Intergranular and intragranular behavior of polycrystalline aggregates. Part 2: Results

Fabrice Barbe, Samuel Forest, Georges Cailletaud *

Centre des Matériaux/UMR 7633, Ecole des Mines de Paris/CNRS, BP87, F-91003 Evry, France

Received in final revised form 16 May 2000

Abstract

The global, intergranular and intragranular responses of a polycrystalline aggregate are investigated. It is shown that the heterogeneity of stress and strain dramatically increases from the global to the local level. Plastic deformation structures develop on a scale larger than the grain. Several types of boundary conditions are applied to polycrystalline aggregates, in order to estimate the importance of the surface effect. The results obtained are presented as contour plots on the cube, and a detailed study is performed to relate the variation obtained with the orientation of the grain and the position in the aggregate.

Keywords: B. Crystal plasticity; B. Elastic-viscoplastic material; B. Polycrystalline material; C. Finite element

1. Introduction

In the first part of the present work (Barbe et al., 2001), a numerical model has been proposed to simulate the mechanical behavior of a polycrystalline aggregate. In the second part, a particular aggregate (*m4*) is depicted in detail, in order to characterise the homogenised response of the material, but also the stress or strain heterogeneity. This heterogeneity can be assessed by applying some averaging operations of the given fields on all the grains with the same crystallographic orientation, on a specific grain, or by considering the local values. It will be shown that the scatter increases dramatically when a local value is considered. Besides, special attention should be paid to the variability of these quantities according to parameters like the volume of a grain, the distance to a free surface or the distance to the grain

* Corresponding author. Tel.: +33-1-6076-30-56; fax: +33-1-60-76-31-50.
E-mail address: gc@mat.ensmp.fr (G. Cailletaud).

0749-6419/01/$ - see front matter
PII: S0749-6419(00)00062-0

boundary. However, a more complete modeling and characterisation of polycrystalline plasticity would require to take into account more parameters. For this purpose the number of grains within the polycrystal and the absolute grain size might be two of the essential parameters. This problem is briefly tackled in Section 3.1.

In Section 2, the conditions of the F.E. calculation are described, and the reference calculation using the self-consistent formalism is performed. After comparing the global loading curves and the stress-strain curves on each phase for these two approaches in Section 3.1, the end of the paper concentrates on the local fields (Section 3) and on the effect of a free surface (Section 4). The plasticity mechanisms are studied through stress and strain fields, but also quantities like the number of active slip systems or the amount of plastic slip. This latter is defined as the sum of the plastic slips over the systems $\left(\sum_s \left|\gamma^s\right|\right)$ so it does not necessarily evolve as an equivalent deformation. Contour plots are shown in Sections 3.3 and 4. The analysis of the surface effect is conducted with representations of the distribution of internal variables on different spaces: along a particular line, on contour plots and with averaged values in planes parallel to the free surface. Several boundary conditions are investigated, in order to extract the surface effect from the local scatter due to stress redistribution: uniaxial tension with four lateral faces left free of forces on the one hand, fully prescribed strain on the other hand, and intermediate cases with only prescribed axial strain. The importance of the surface effect can then be qualified by comparing it to the intergranular redistribution.

The motivation of such a study has to be found in the literature, specially in articles dealing with the study of the surface effect from a metallurgical point of view. Extensive transmission electron microscopy studies of deformed single crystals at the applied stress-state of early works (Fourie, 1967; Mughrabi, 1970; Pangborn et al., 1981; Ungar et al., 1982) showed the propensity of the near surface region to harden with dislocation arrangements and densities different from those observed in the crystal interior. Still the effects observed are controversial (Mughrabi, 1992): a *hardened surface* layer was found in experiments on copper (Pangborn et al., 1981); the change in mechanical properties was related to the dislocation density, which was higher than in the bulk of the crystals. Besides, other works (Fourie, 1967; Mughrabi, 1970) displayed the inverse effects of a *softening surface* region where dislocation densities are lower and cell dimension larger than in the crystal interior. In the case of multiple slip (Ungar et al., 1982), no conclusion could be drawn. Actually, the experimental study of such an effect is a very difficult task. The observations can be modified due to the presence of the oxide layer, which may introduce local overstress. This explanation was for instance proposed by some authors (Nakada and Chalmers, 1964) after tests on aluminium and gold single crystals: the surface film is work-hardened for aluminium (where an alumina layer is present), but not on gold. Similarly, the conclusions on single crystals can be different from those on polycrystals. The mechanical approach can bring new results, which can be helpful for the general discussion. Note that the calculations are performed with a crystallographic model, which means that slip is the only deformation mechanism. Accordingly, the effect of the local orientation will be significant. Still, the model properties are independent of the distance to the surface, or of the distance to the

grain boundaries. The effect which can appear in the computation at the level of the integration point has to be related to the local balance of momentum, and to the local stress redistribution. There is no specific effect like dislocation pile-up, image force. The purpose of the modeling is precisely to address the question of the reliability of the mechanics as it is applied at the microstructural scale.

Other attempts have recently been made to evaluate the surface effect numerically (Pilvin, 1998; Sauzay and Gilormini, 1999; Barbe et al., 1999). While the first two approaches consider a crystallographic inclusion in a homogeneous semi-infinite medium, in the third, the analysis is based on finite element simulations of polycrystalline aggregates. The work of Pilvin enables to characterise a new concentration rule, for evaluating the stress in the inclusion, depending on the distance to the surface. Due to the decrease of the constraint near to the surface, the concentration rule tends to a Reuss type model while the strain heterogeneity increases. The perturbation due to the surface approximately corresponds to 3 or 4 grains in depth. The work of Sauzay and Gilormini considers cyclic loadings, but is restricted to an elastic homogeneous medium, having in view high cycle fatigue modeling. With only one slip system in the inclusion it is shown that the surface effect strongly depends on the crystal orientation. These conclusions may have to be revisited when the influence of a realistic local microstructure is introduced.

2. Conditions of the calculations

The aggregate called *m4-200-200* (Barbe et al., 2001) is now studied in detail, with a $18\times18\times18$-element-mesh, as justified in Part 1 of the article. It contains 200 grains randomly oriented. The geometry of the microstructure is represented with finite elements in Fig. 6c of the first part and the material parameters are given in Section 3.2 of the first part.

In the following sections the type of boundary conditions is systematically specified. It is one of the four loading cases defined below:

- *homogeneous strain boundary* conditions (HSB), corresponding to a prescribed mean deformation $\underset{\sim}{\mathbf{E}}$ of the aggregate. All components of the displacement vector at each node (position $\underline{\mathbf{x}}$) of the outer boundary of the cube are prescribed according to:

$$\underline{\mathbf{u}} = \underset{\sim}{\mathbf{E}}.\underline{\mathbf{x}} \;\Rightarrow <\varepsilon> = \underset{\sim}{\mathbf{E}} \tag{1}$$

This prescribed strain $\underset{\sim}{\mathbf{E}}$ is obtained from the BZ homogenisation model (Berveiller and Zaoui, 1979) presented in Part 1. The model is integrated in uniaxial tension, that is under prescribed axial strain and a null stress on all the other components. This should also lead to a zero resulting force on the lateral faces if the F.E. computation is in agreement with the BZ model.

- a *mixed* type of *boundary* conditions (MB), where normal displacements are imposed to the faces of the cube. The in-plane displacements of the faces are

thus let free. These normal displacements correspond to the prescribed strain $\underset{\sim}{\mathbf{E}}$.

- *one* lateral *free face* (1FF), where the axial displacement is imposed on the top and bottom faces, and three of the four lateral faces are subjected to the prescribed normal displacement defined above,
- *four* lateral *free faces* (4FF), where the axial displacement is imposed only on the top and bottom faces.

A comparison of the local behavior according to the load case is detailed in Section 4. Fig. 1 allows a first comparison on a macroscale.

3. Results

3.1. Global scale

Since random orientations have been assigned to the grains in the aggregate *m4-200-200* under concern here, each grain is considered as a new phase. It can be seen in Fig. 1 that the agreement between the mean values obtained from the F.E. analysis and the prediction of the homogenisation model is good. The BZ curve obtained with the RVE simulation exactly fits the response of the F.E. HSB calculation. As expected, the F.E. response is softer and softer when the boundary conditions are released: at the end of the tensile load, the axial stress value is 396.3 MPa with the BZ model, 395.4 MPa with HSB, 384.5 MPa with MB, then 375.3 MPa for 1FF and 368.3 MPa for 4FF. The maximum difference between the different types of load is then 7%. The fact that the variation of the overall response remains reasonably low indicates that the considered volume element containing 200 grains with random orientations is not far from being a representative volume element (RVE) as defined in the homogenisation theory (Huet, 1990).

The question of the minimum size of a RVE for a polycrystalline aggregate remains a central and unsolved question of the mechanics of heterogeneous materials. Actually the answer depends on the loading conditions and on the texture of the material. The present numerical tool can be used to study the transition from the multicrystal to the actual polycrystal behavior. If the number of grains is not large enough, several realisations of the distribution must be considered, as done in the Part 1. Such a transition has been studied for the torsion of copper wires (Quilici et al., 1998): a typical number of 1000 grains in the cross-section of a cylindrical specimen has been found, that is about 30 grains in the diameter. The polycrystalline cube considered here is made of a smaller number of grains but is not far from being a RVE at least for tensile overall loading conditions.

Moreover, as shown in Fig. 1b, the tensile tests responses in the x direction for the four cases of boundary conditions all fall onto the responses in the perpendicular y direction, which confirms the isotropic behavior of the bulk. Thus it is demonstrated that the self-consistent modeling is reasonable when 200 grains are involved in an aggregate, and that the aggregate can be considered approximately as isotropic. More complex loading conditions should be applied to the aggregate to confirm the isotropic nature of the overall material response.

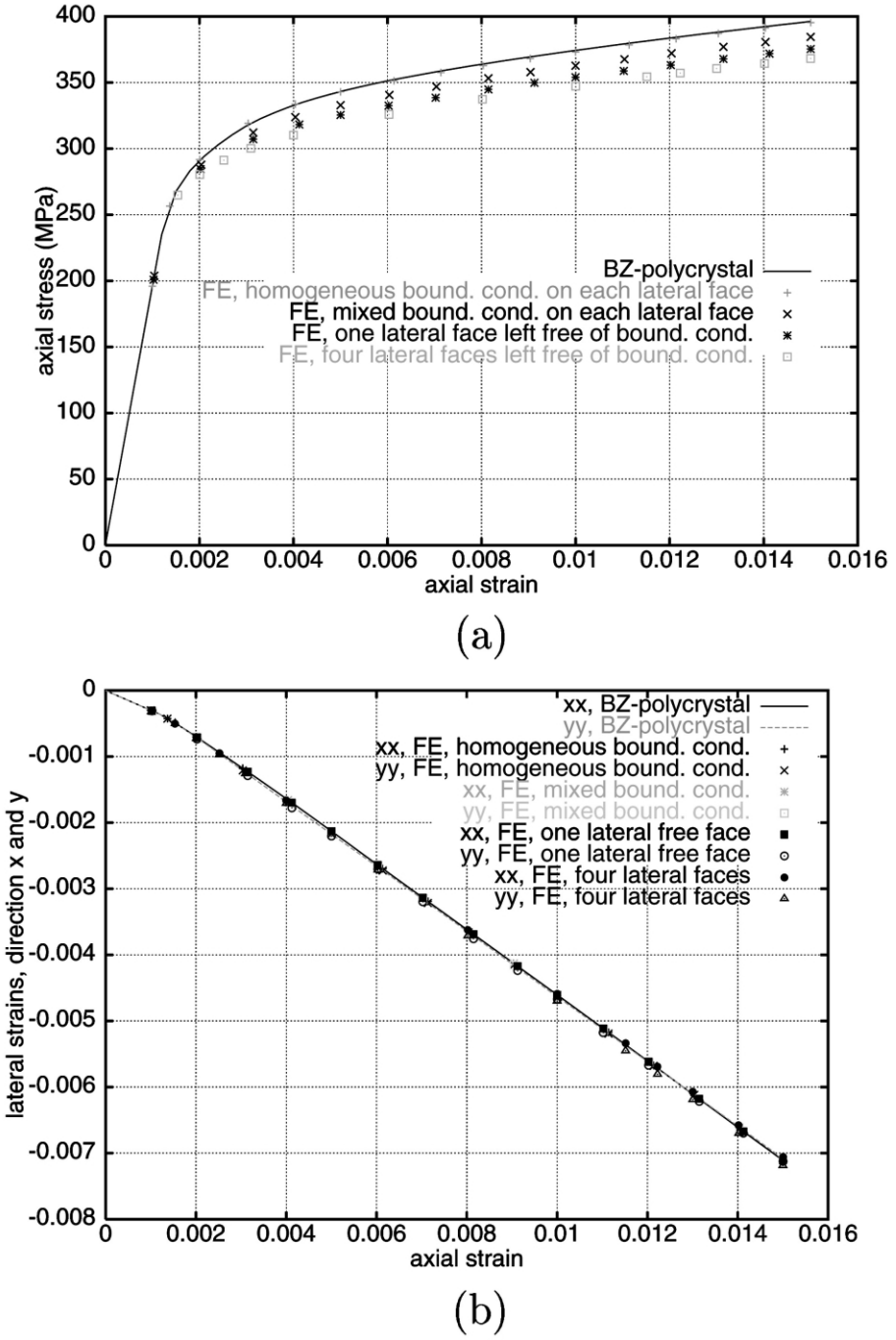

Fig. 1. Simulations of tensile tests to 1.5% axial strain, from BZ-homogenisation and F.E., with different loading conditions: (a) axial stress vs axial strain, (b) lateral strains vs axial strain.

3.2. Phase scale

The averaged responses of the grains are quite inhomogeneous. As shown in Fig. 2c,e where the mean stress–strain behavior of each of the 200 grains is plotted, some phases work in tension as imposed by the global load, whereas others work in compression as soon as plastic strain occurs. This is a direct consequence of the interaction between grains; in such a configuration the response does not depend only on the crystallographic orientation but predominantly on the constraints due to neighboring grains, until the overall applied deformation affects once again the compressing regions. All the phases then work in tension. It is also worth noting how scattered those curves are, in comparison with the mean stress–strain response and with the behavior of each of the four basic orientations (cf Part 1 of the article). This interaction between grains leads to strongly non-proportional mean stress evolution, as demonstrated on the $(\sigma_{yy} - \sigma_{zz})$ plane on Fig. 3. Since the grain elasticity is chosen isotropic, all the grains are equivalent up to the onset of plasticity, at $(\sigma_{yy} = -74$ MPa, $\sigma_{zz} = 148$ MPa), then the plastic flow produces contradictory evolutions according to the grain: the lateral stress σ_{yy} can either increase or decrease.

The major role played by the neighboring grains on the behavior of an individual grain can be assigned to the number of surrounding grains: from ten to twenty grains differing from their size, morphology, position in the bulk and orientation, that is ten to twenty ways to behave. A first classification of the grains is made according to their volume in Figs. 4a and 5a. The final state of all the grains is shown in Fig. 4a, together with the macroscopic curves. The symbol chosen for each grain depends on its volume (respectively less than 3, between 3 and 30, more than 30, in all simulations the volume of 1 element is taken equal to 1), in order to check if there is a numerical artefact due to the small size grains. It is observed that the smallest grains present the biggest discrepancy with respect to the reference state. Such a spreading might also be due to the influence of a surface: as seen in Fig. 4b the smallest grains are often the closest to the surface. However, if the smallest grains are excluded from the analysis, the variation remains large ($\pm 30\%$) for grains having a volume superior to 27, i.e. for grains described by $27 \times 27 = 729$ integration points. This variation characterises the neighborhood effect, and the grain-to-grain interaction. It is also illustrated in Fig. 5a and b where grains are also classified according to their normed axial stress and their distance to the surface. The normed stress is defined by the ratio of the stress from F.E. divided by the stress from the homogenisation model. The variation is quantified by the width of the cloud of points at a given height of the diagram. For example, grains in the core of the aggregate (respectively the biggest grains), behave nearly as predicted by the homogenisation model. But as soon as a grain nearer the surface is considered (respectively a smaller grain), a larger dispersion of behaviors is displayed. Since the behavior of the grains in the near surface region have proved to be particularly influenced by their neighbors and because of the controversy on that subject exposed in the literature, a study is conducted in Section 4 on the effect of the boundary conditions for a tensile test, which is specifically a study of the free surface effect in a purely mechanical sense.

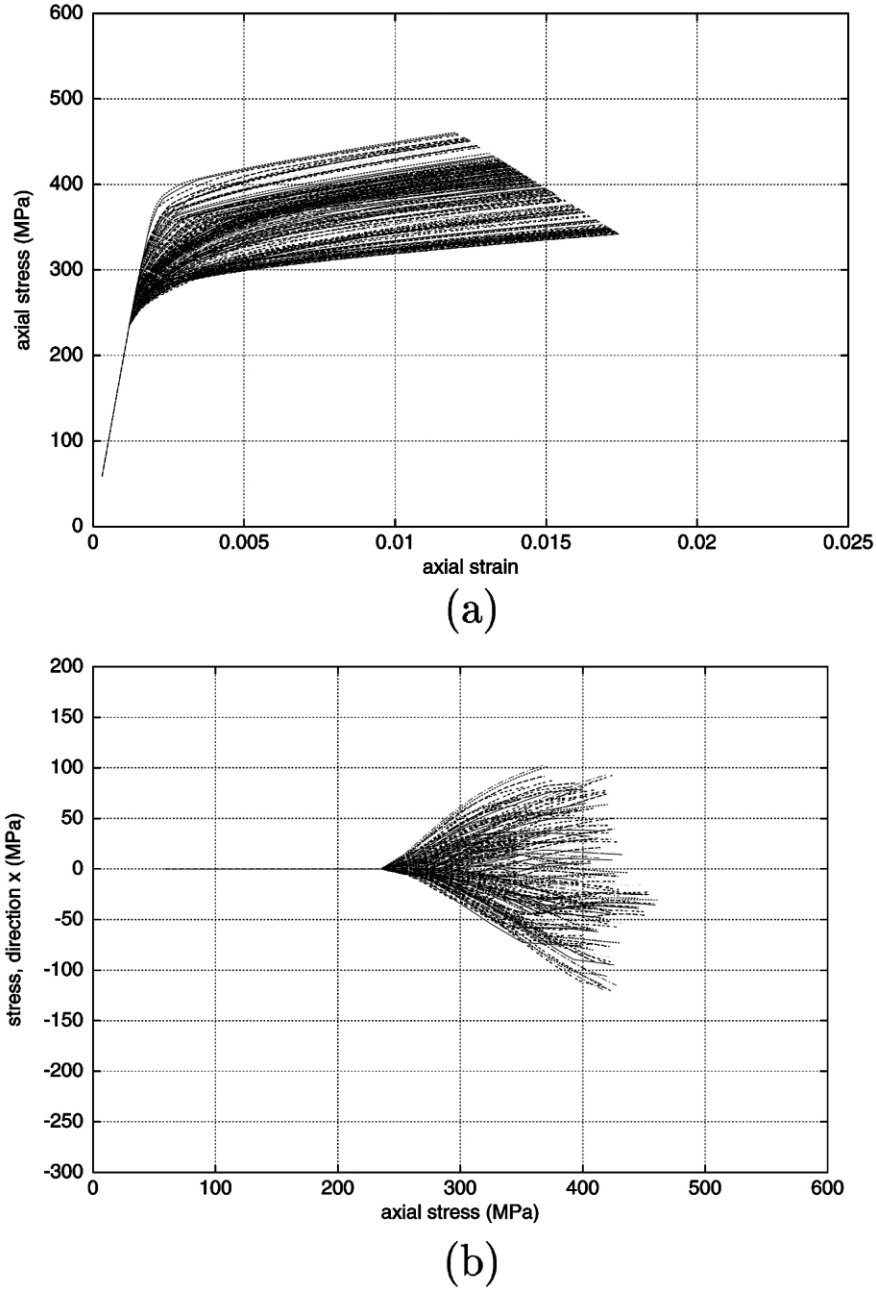

Fig. 2. Illustration of inter- and intra-granular heterogeneity from the mean response of each of the 200 grains of the polycrystal: (a,b) BZ-homogenisation; (c,d) F.E. HSB; (e,f) F.E. 4FF; (top) σ_{zz} vs ϵ_{zz}, (bottom) σ_{xx} vs σ_{zz} (*continued on next page*).

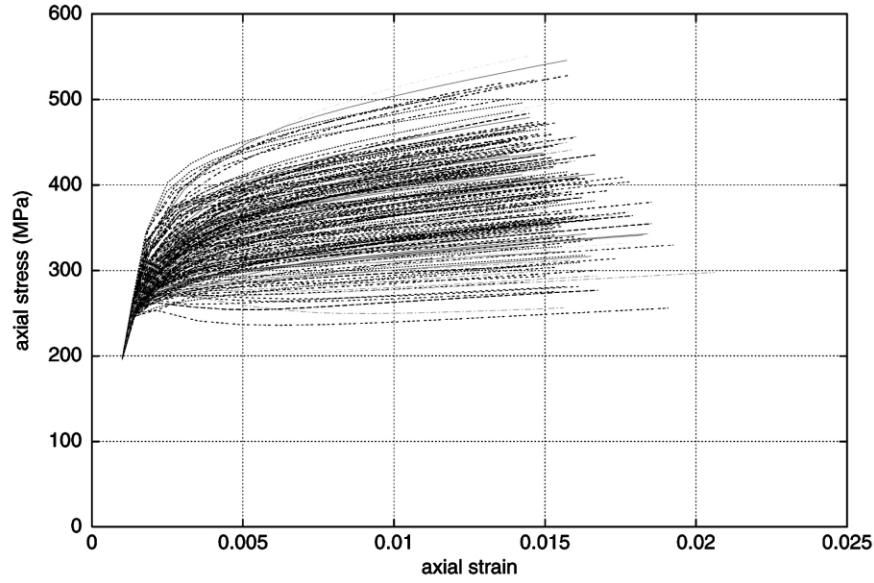

(c)

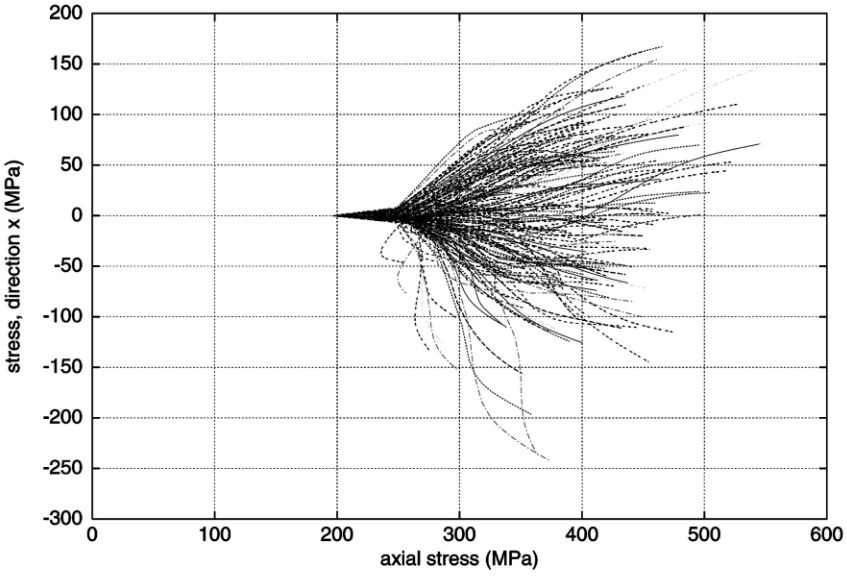

(d)

Fig. 2. (*continued on next page*)

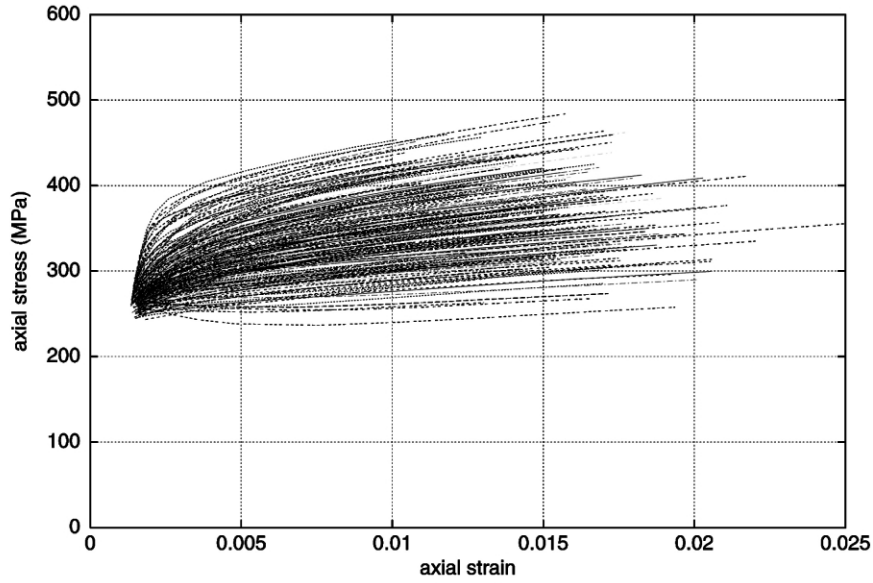

(e)

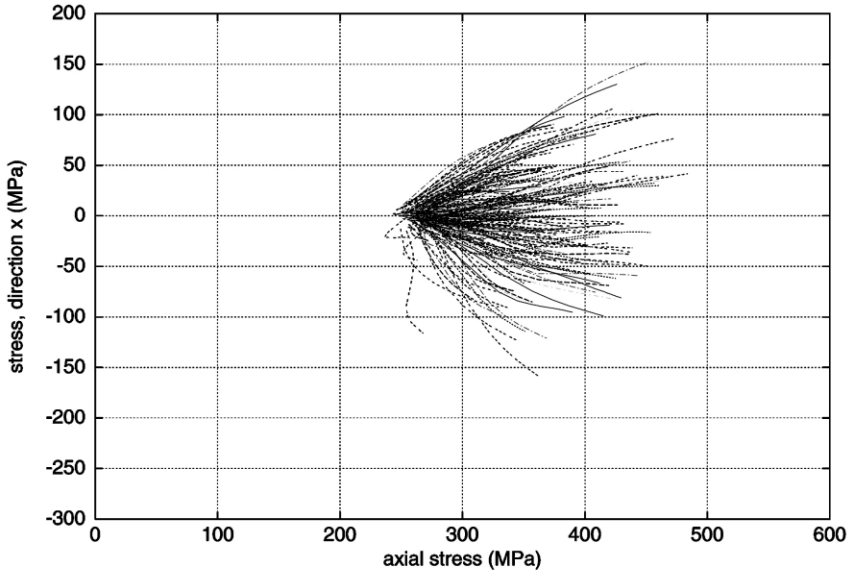

(f)

Fig. 2. (*continued*)

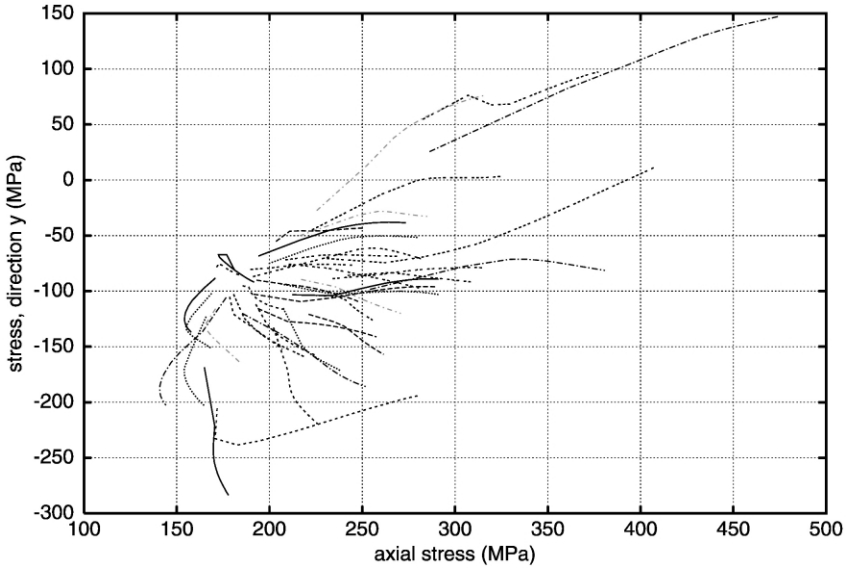

Fig. 3. Mean stress paths in each of the 200 phases of the polycrystal tensile strained at 1.5% with isovolumic conditions.

3.3. Intragranular level

After considering the heterogeneity at the scale of the phases, the final step of the analysis of the F.E. results concerns the Gauss points. Three main features result from the observation of the plastic strain fields in the aggregate (Figs. 6 and 7):

3.3.1. Development of plastic deformation structures

The plastic deformation distribution in an aggregate is generally not dictated by the given geometry of the microstructure. In particular, the geometry of grain boundaries does not directly appear on the contour plots (see e.g. Fig. 7a and b that feature the distribution of cumulated strain on slices taken in the core of the bulk or see Fig. 12 reporting the distribution of plastic slip on an external face of the aggregate). In contrast, deformation meso-structures develop like deformation bands that go across several grains. Percolated dissipation structures seem to find their way through the random distribution of grains. Those features can be observed with better accuracy on the contour of *m4* discretised into $24\times24\times24$ quadratic elements presented in Part 1 of the article. If the kinematic hardening term is removed from the constitutive laws, similar internal deformation structures form on the contour as well as in the interior. Two pieces of information are then confirmed: (i) the meso-structures of deformation develop at the earliest stages of plastic slip; (ii) with $72\times72\times72=373248$ integration points to represent the microstructure containing 200 grains, the convergence in the thickness and refinement of the meso-structures does not seem to be attained.

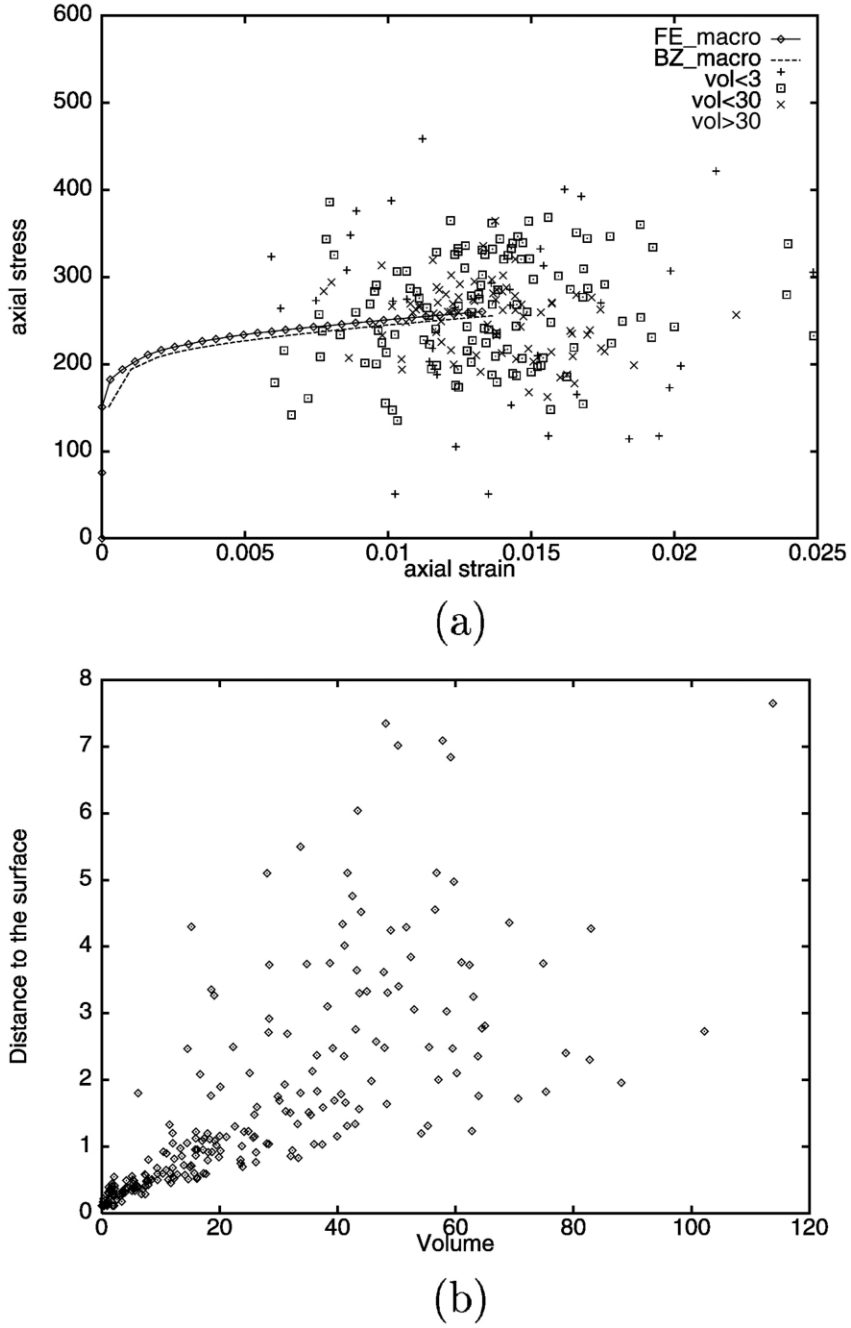

Fig. 4. (a) Final state in the stress–strain plane for all the grains according to their volume, (b) volume of the grain vs distance to the surface of the aggregate.

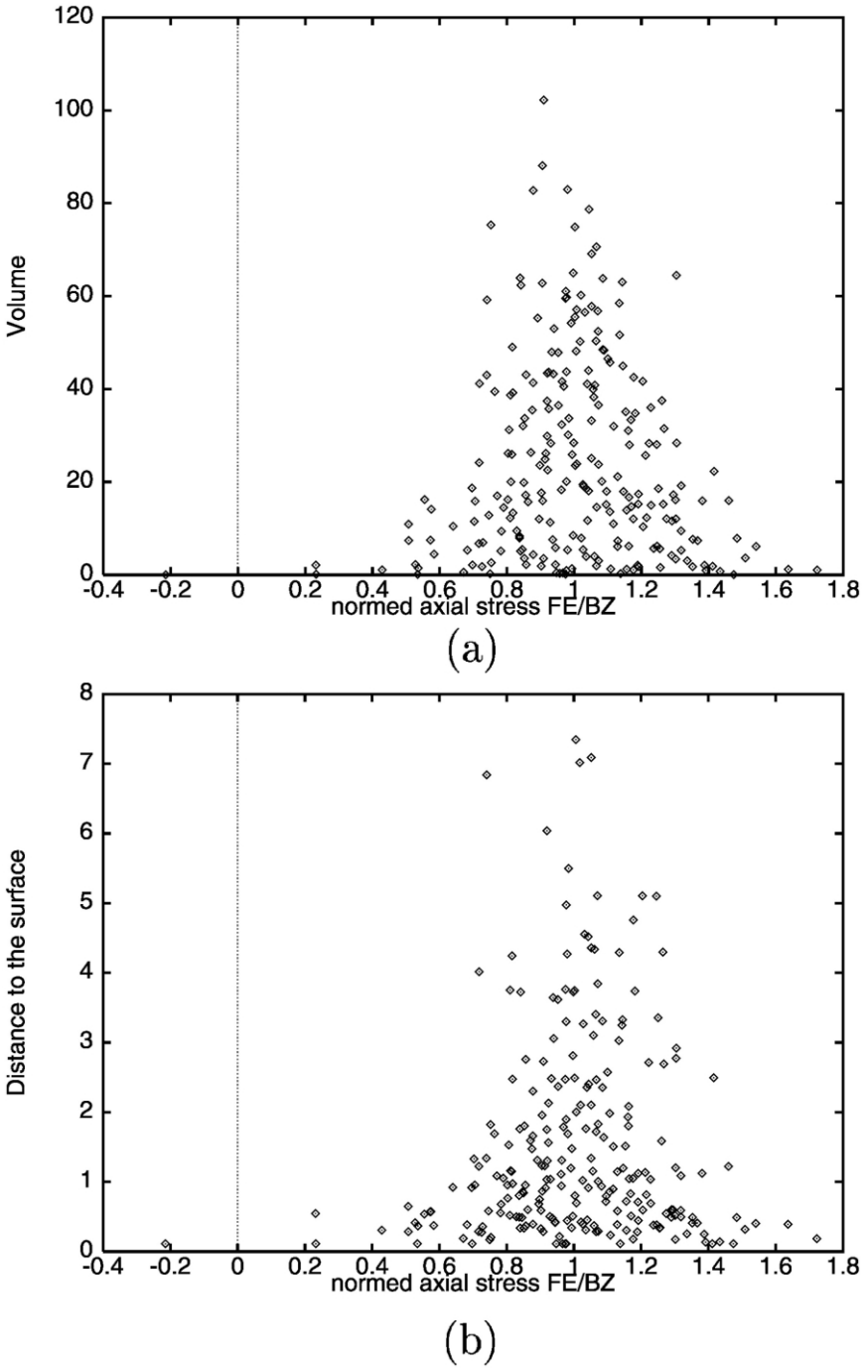

Fig. 5. Stress heterogeneity between the grains according to (a) their volume, (b) their distance to the surface.

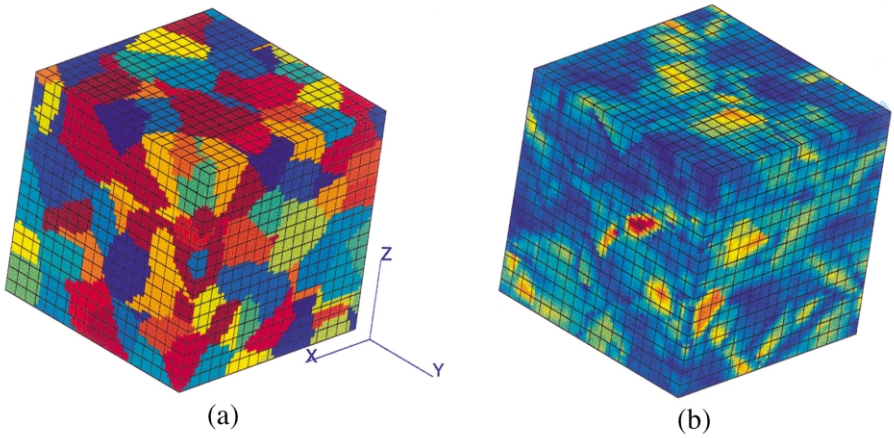

Fig. 6. (a) Grain map, (b) contour of the norm of the lattice rotation vector at the onset of plastic deformation.

3.3.2. Direct effects of grain boundaries

In the contour plots of some specific variables, the shape of the grain boundaries can be clearly seen. This is the case for instance for the resolved shear stress or for the number of active slip systems, as shown previously (Quilici and Cailletaud, 1999). Interestingly, the distribution of lattice rotation also reveals the grain boundaries. For that purpose, the model of single crystal plasticity used in this work has been extended to include effects of small rotations. The gradient of the velocity field is divided into symmetric and skew-symmetric parts according to:

$$\dot{u}_{ij} = \dot{\varepsilon}_{ij} + \omega_{ij} \tag{2}$$

$$\omega_{ij} = \omega^e_{ij} + \omega^p_{ij} \quad \text{with} \quad \omega^p_{ij} = \sum_s \frac{1}{2}\dot{\gamma}^s\left(m^s_i n^s_j - m^s_j n^s_i\right) \tag{3}$$

The elastic part ω^e_{ij} accounts for the lattice rotation rate with respect to the reference space frame and, as a skew-symmetric tensor, can be represented by a pseudo-vector and integrated. The local redistribution of the norm of the lattice rotation vector around the grain boundaries is shown in Fig. 6. Lattice rotation can be maximum near the boundary or in the core of the grain, but the lattice curvature associated with the gradient of the lattice rotation vector is always maximum near the grain boundaries.

3.3.3. Intragranular stress state

The overall integration points of one grain are considered in Fig. 8; their response is given at three strains ($E = 0.5$, 1.0 and 1.5%), together with the mean response of the grain and the response of a single crystal having the same orientation in tension up to 1.5%. The local stress–strain curve shows again more and more scatter; even

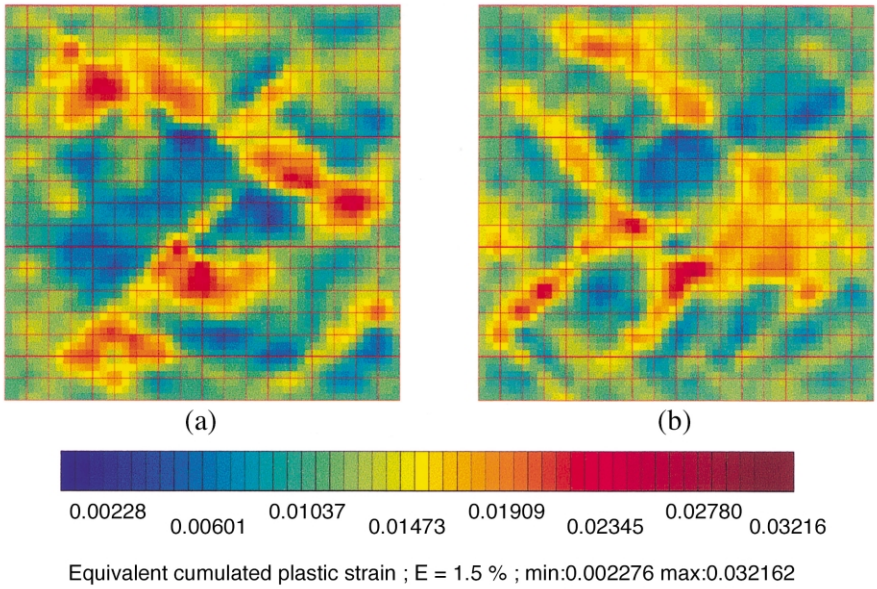

Fig. 7. Contour of the equivalent cumulated plastic strain on two slices of the interior bulk: (a) slice perpendicular to the x axis, (b) slice perpendicular to the y axis.

under macroscopic tensile load, the local stress in the tensile direction can be compressive at some locations of the aggregate. The range of intergranular heterogeneity can be compared to the range of intragranular heterogeneity: the mean responses of all the grains in polycrystal (*m4-200-200*) are plotted with the same scale as the responses of the integration points within the biggest grain (*grain58*) of the microstructure. On the axial stress–strain curves, the range of heterogeneity is greatly more pronounced among points within a grain than among grains within a polycrystal. In the latter case, the averaging effect partially erases the local variations. Obviously the points within a multiphase structural element (element with several crystallographic orientations assigned to the integration points) need to be excluded from the analysis because the way their behavior is affected by the neighboring points is still obscure. However, as seen in Fig. 9, which corresponds to a grain containing less integration points, the heterogeneous behavior remains characteristic of the intragranular behavior and the range of heterogeneity is still comparable to that observed with mean responses of grains within the polycrystal (Fig. 2c,e). It highlights the fact that the heterogeneity within a grain, produced mostly by the neighboring mechanical constraints, could be a clue in the modeling of damage in polycrystalline aggregates.

The difference in the behavior within a grain in comparison with the one within a polycrystal is emphasised when considering the local stress paths. Figs. 8 and 9 display the typical stress path observed in *grain58:* as a matter of fact, the lateral stress σ_{xx} and the axial stress σ_{zz} seem to be related by a simple expression like:

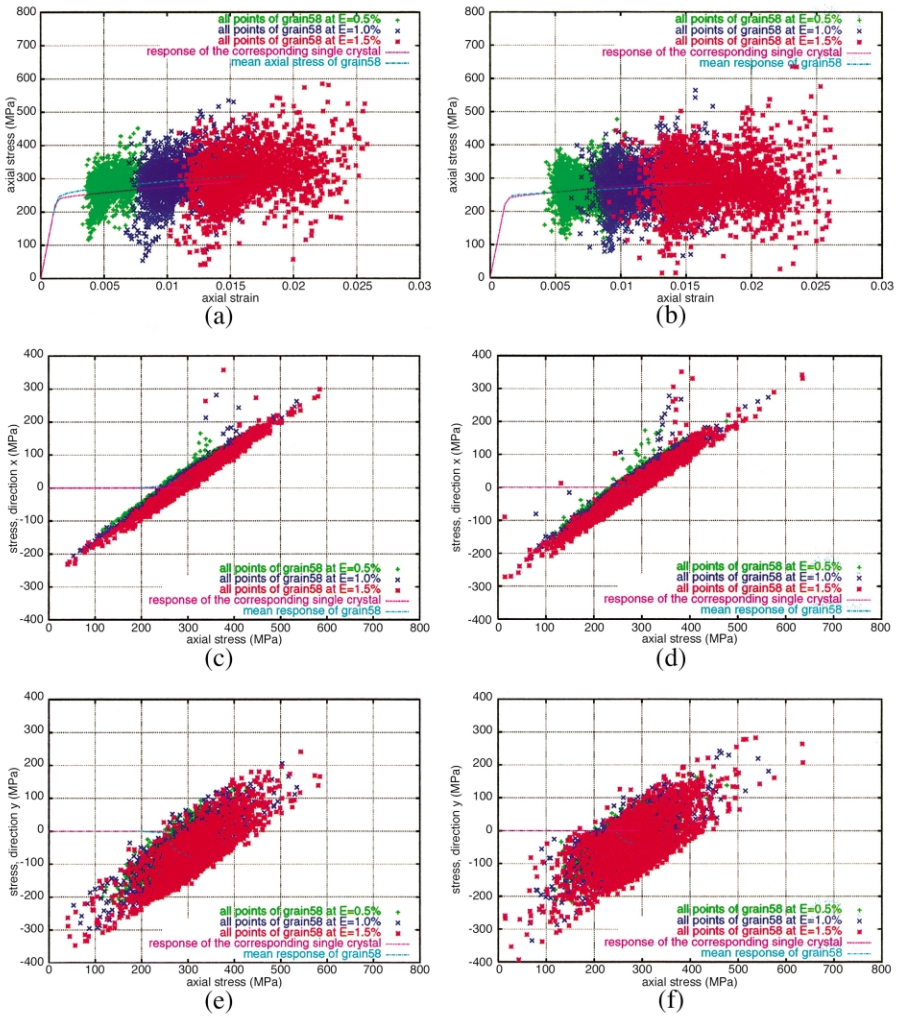

Fig. 8. Intragranular heterogeneity and effect of the free surface: responses at three strains ($E = 0.5$, 1.0 and 1.5%) of all the points within *grain58* (2265 points); (a, b) σ_{zz} vs ϵ_{zz}; (c, d) σ_{xx} vs σ_{zz}; (e, f) σ_{yy} vs σ_{zz} (left) case F.E. HSB, (right) case F.E. 4FF.

$$\sigma_{zz} - \sigma_{xx} = \sigma_Y \tag{4}$$

where σ_Y refers to the actual yielding stress, which increases as the load is applied. This is particularly well illustrated if only three strains of the load are represented ($E = 0.5$, 1.0 and 1.5%). As the deformation proceeds and as the elastic limit is raised, the line of gradient equal to 1 follows the mean response of the grain by moving to the right. This curve should be replotted in terms of principal stresses, to

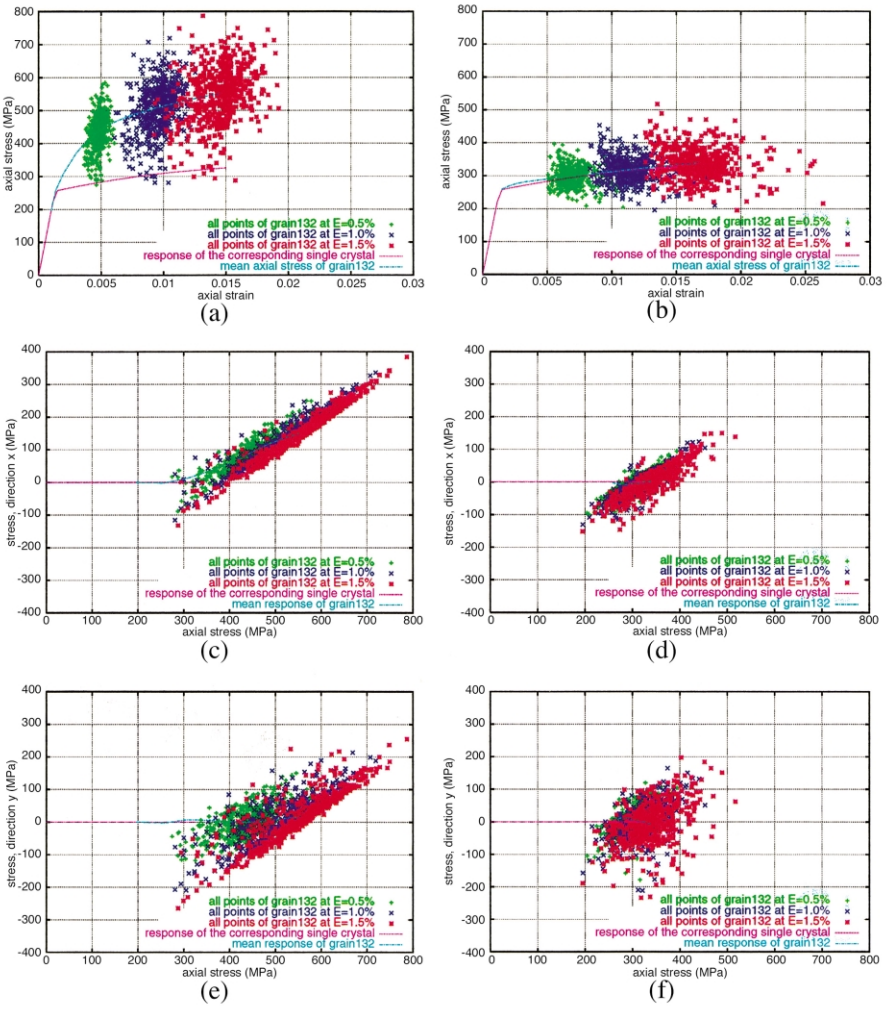

Fig. 9. Intragranular heterogeneity and effect of the free surface: responses at three strains ($E = 0.5$, 1.0 and 1.5%) of all the points within *grain132* (545 points); (a, b) σ_{zz} vs ϵ_{zz}; (c, d) σ_{xx} vs σ_{zz}; (e, f) σ_{yy} vs σ_{zz}; (left) case F.E. HSB, (right) case F.E. 4FF.

fit with Tresca criterion. But, even in the present form, it highlights the constraint effect in the grains, leading to 3D fields, and it is typical of the local behavior of each point. Yet, because of the scale transition which produces additional hardening, this relation is not valid anymore concerning the mean stress paths in the grains within a polycrystal, as shown in Fig. 2b,d and f. This observation is true either for the behavior predicted by the homogenisation model or for the mean behavior per grain issued from F.E.

4. The free surface effect

4.1. Phase scale

Comparison of the effective stress–strain curves from the four loading conditions was given in Fig. 1 and showed a maximum difference of 7% between the extremal cases of HSB and 4FF. The comparison between those two extremal cases is now transferred to the level of the grains in Fig. 2: the mean responses in each grain, according to BZ-homogenisation model, F.E. HSB and F.E. 4FF respectively are plotted. The case of HSB displays the most heterogeneous intergranular behavior, on the axial stress–strain curves as well as on the loading paths expressed with stresses. To quantify the difference in the range of heterogeneity, the maximum stress–strain response in each case has been extracted and compared with F.E. HSB. Note that the most hardened grain in the case of HSB is not the most hardened in the BZ-polycrystal, neither in the case 4FF. Anyway, the purpose is not to identify and characterise the grains individually but only to evaluate the discrepancy between different simulations of tensile test as the scales of representation are refined (from macro to micro via meso). So, the maximum response obtained with BZ-polycrystal differs from the one of F.E. HSB by -16.4% whereas the one of F.E. 4FF differs by -12.2%. About the minimum responses, the difference reaches $+33.72\%$ in the case of BZ-polycrystal and stands at $+0.75\%$ in the case of 4FF.

Thus the comparison at this scale allows us to calibrate the limitations of the homogenisation model with the assumption of uniform fields in the phases: despite the very good agreement at the global scale (0.22% on the axial stress at 1.5% axial strain), the fields in the actual material reflect disordered behaviors among grains that cannot be captured with the simplified model; for instance, on Fig. 2a the distribution of the axial stresses on a line of gradient equal to $\alpha \times \mu$ [α and μ being defined in the transition rule (9) in part 1 of the article] at the end of the load is valid on average for many orientations, but may be inadequate to represent the real behavior of an individual grain with the same orientation.

4.2. Analysis in planes parallel to a free surface

The behavior is represented according to the distance to a lateral free face ($y = 0$) in Fig. 10. This face is free for the case 1FF, and for 4FF, and is submitted to the conditions defined in Section 2 for HSB and MB. Several types of variables are averaged in planes parallel to that lateral face. The effect of the applied boundary conditions can then be checked on average, independently of the local variation due to the environment of each grain. The von Mises stress (Fig. 10a) is lower by 12% in case 4FF than in case HSB near the surface region; it also has to be noted that MB case is not far from 1FF and 4FF cases: letting free the in-plane displacements on the lateral sides of the cube produces a significant stress relaxation. The von Mises strain $[((2/3)\underset{\sim}{\varepsilon}^p : \underset{\sim}{\varepsilon}^p)^{0.5}]$ (Fig. 10b) and the cumulated plastic strain $[\int (2/3)\dot{\underset{\sim}{\varepsilon}}^p : \dot{\underset{\sim}{\varepsilon}}^p)^{0.5} \mathrm{d}t]$ (Fig. 10d), which respectively quantify the actual plastic strain state and the length of the macroscopic plastic strain path, give the same information. They show

that the strain is lower for the case of constraint boundary conditions (20% lower near the surface for HSB compared to 4FF). Fig. 10c shows the evolution of the amount of plastic slip: it is defined as the sum of the slip over the systems ($\sum_s |\gamma^s|$). Contrary to the deformation, it is bigger near the surface for HSB than for the other cases. The fact that more plastic slip finally induces less strain for HSB can be explained by Fig. 10e and f, which demonstrates that the value of the larger slip (Fig. 10e) is lower for HSB, and that the number of slip systems (Fig. 10f) is larger, leading to a competition between the systems. In the case of free boundaries, the predominant slip benefits from "more space" to develop, and produces important strain, whereas in the case HSB, the action of predominant slip remains limited by the other systems, which develop to reduce strain incompatibilities.

Considered altogether, those effects, which appear to be the same on either side of the aggregate, lead to the observation of *softened free surfaces* where both axial stress and plastic slip proved to be lower in the near surface region when no condition is imposed to this surface. Besides, the free surface enables the loading paths in its neighborhood to be more proportional than in the case of a surface with homogeneous strain conditions.

4.3. Analysis in particular grains

The previous remarks can be made for particular grains studied in Fig. 8 and 9. They show the response at each point of (i) the biggest grain of the aggregate (*grain58* described with 2265 points) and (ii) the most hardened grain (*grain132*). The average number of active slip systems in these grains has been counted: they are defined as the systems where cumulated slip has exceeded 0.00001 during the tensile test. The maximum cumulated slip averaged in those grains are also given in Table 1. The behavior of those particular grains is compared to the one of the single crystals with the same orientations. The agreement about the average amount of cumulated slip in *grain58* is admittedly good: this grain is very large so there might be some places of the grain which are not influenced by its neighbors; furthermore, due to its position in the core of the aggregate, it is surrounded by a large number of grains with different orientations thus forming a quasi-homogeneous surrounding medium, as in the self-consistent scheme. But the number of active slip systems fails to be reproduced when the crystal is embedded in the aggregate. About *grain132,* there is no comparison to be made. The grain is too close to the boundary and too small to be associated to the behavior of the single crystal. However, a direct effect of the interaction with a free surface lies in the number of activated slip systems depending on the loading condition studied: whereas only 5 systems contribute to the deformation in the case 4FF, 8 slip systems are required for the accommodation of the deformation of the grain under HSB.

4.4. Analysis on a line perpendicular to the free surface

The analysis is then pursued deeper into the microstructure: the evolution of the local strains along the integration points of a straight line going from a lateral side

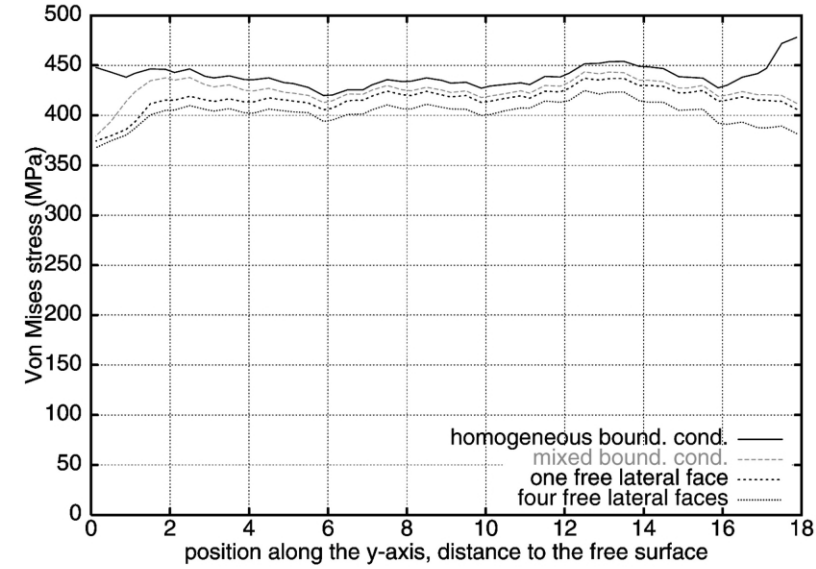

(a)

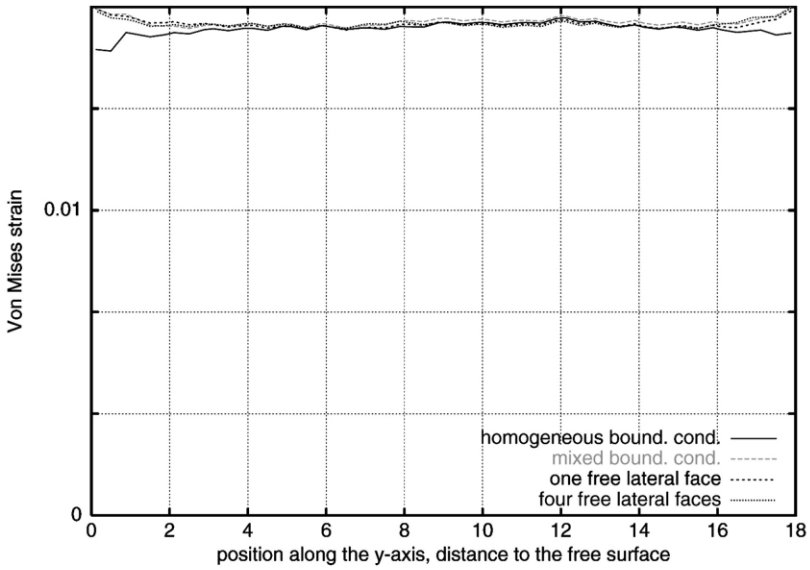

(b)

Fig. 10. Variables averaged in planes parallel to a lateral face of the polycrystal in the four cases of load: (a) equivalent stress; (b) equivalent strain; (c) amount of plastic slip; (d) equivalent cumulated plastic strain; (e) maximum plastic slip over the 12 systems; (f) number of slip systems whose plastic slip exceeds 0.001 (*continued on next one*).

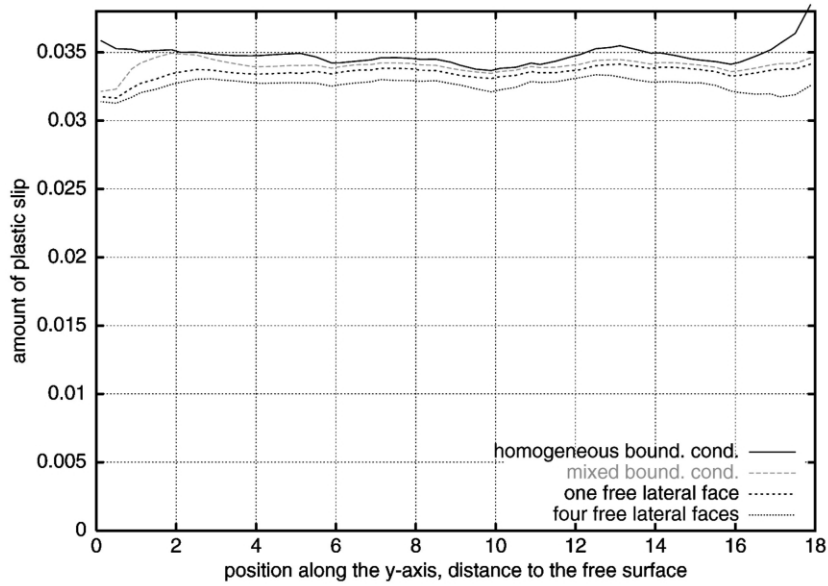

(c)

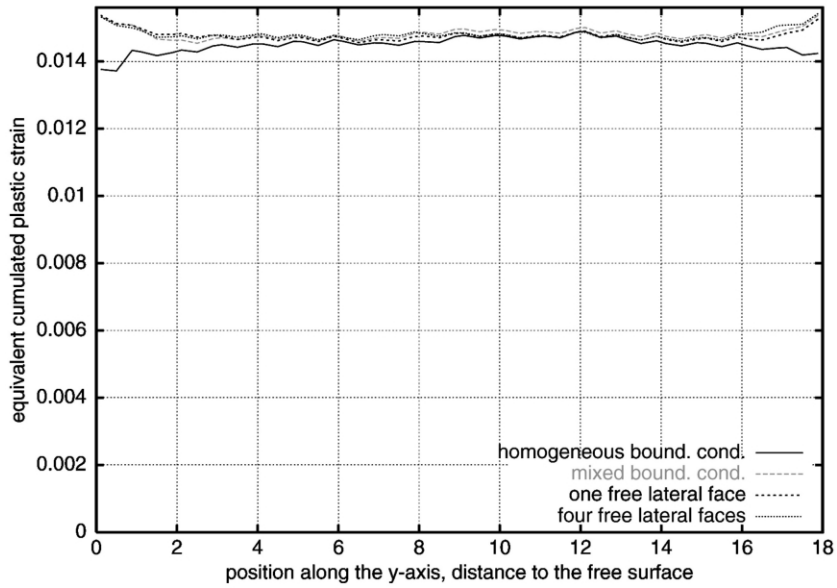

(d)

Fig. 10. (*continued on next page*)

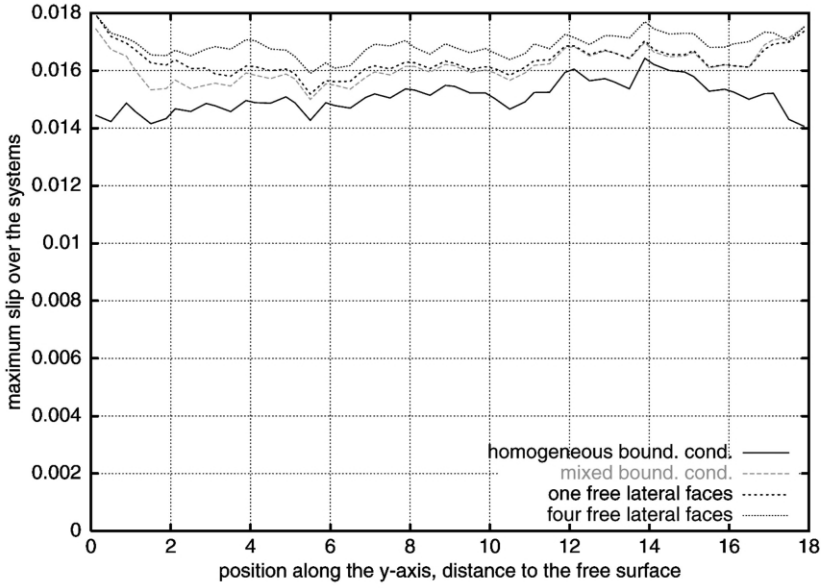

(e)

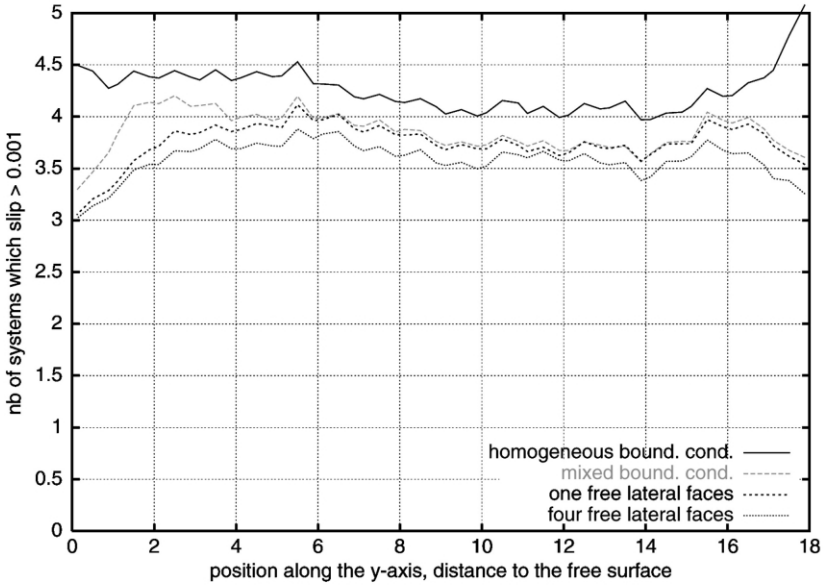

(f)

Fig. 10. (*continued*)

of the bulk to the other is shown in Fig. 11. Considering the amount of plastic slip, we can deduce that (i) the intergranular compatibility forces the grain boundary region to deform more than the core of the grain, (ii) the deformation pattern in some grains is predominantly influenced by the neighboring grains, more than by the crystallographic orientation, (iii) the interaction with the boundaries of the bulk is of the same order as the effect of a free surface (about 20%) since the discrepancy between two cases of load in F.E. is of the same order as the difference between the response of the homogenisation model and the response of the F.E. computations.

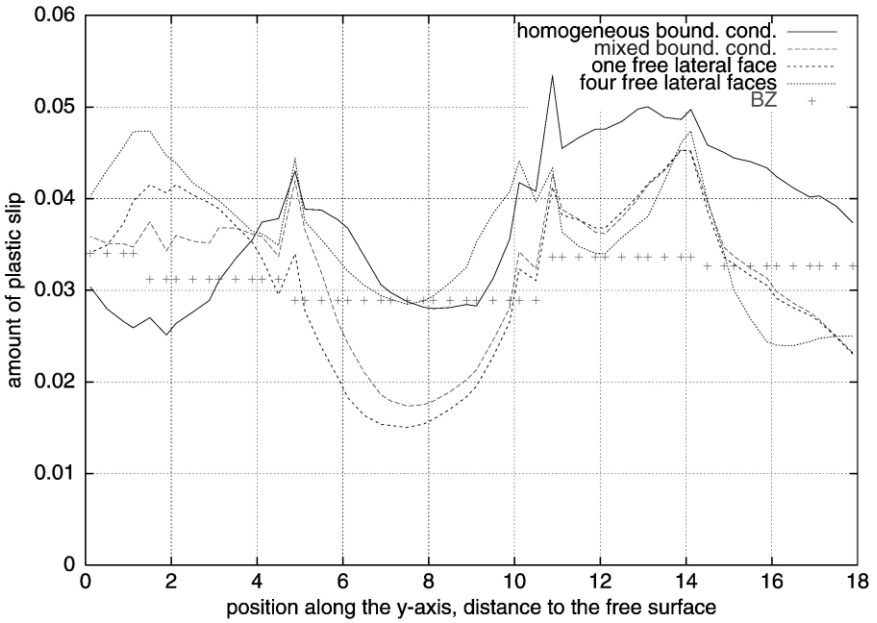

Fig. 11. Evolution of the amount of plastic slip on a line perpendicular to the free surface of the polycrystal in the four cases of load; the line is located in the core and goes from side to side.

Table 1
Effect of the free surface on the mean behavior in particular grains: number of active slip systems together with the maximum cumulated slip

Case of load	*Grain58* (the biggest)	*Grain132* (the hardest)
Single crystal	2 0.0164	3 0.0259
Polycrystal HSB	10 0.0138	8 0.01388
Polycrystal 4FF	10 0.0156	5 0.0184

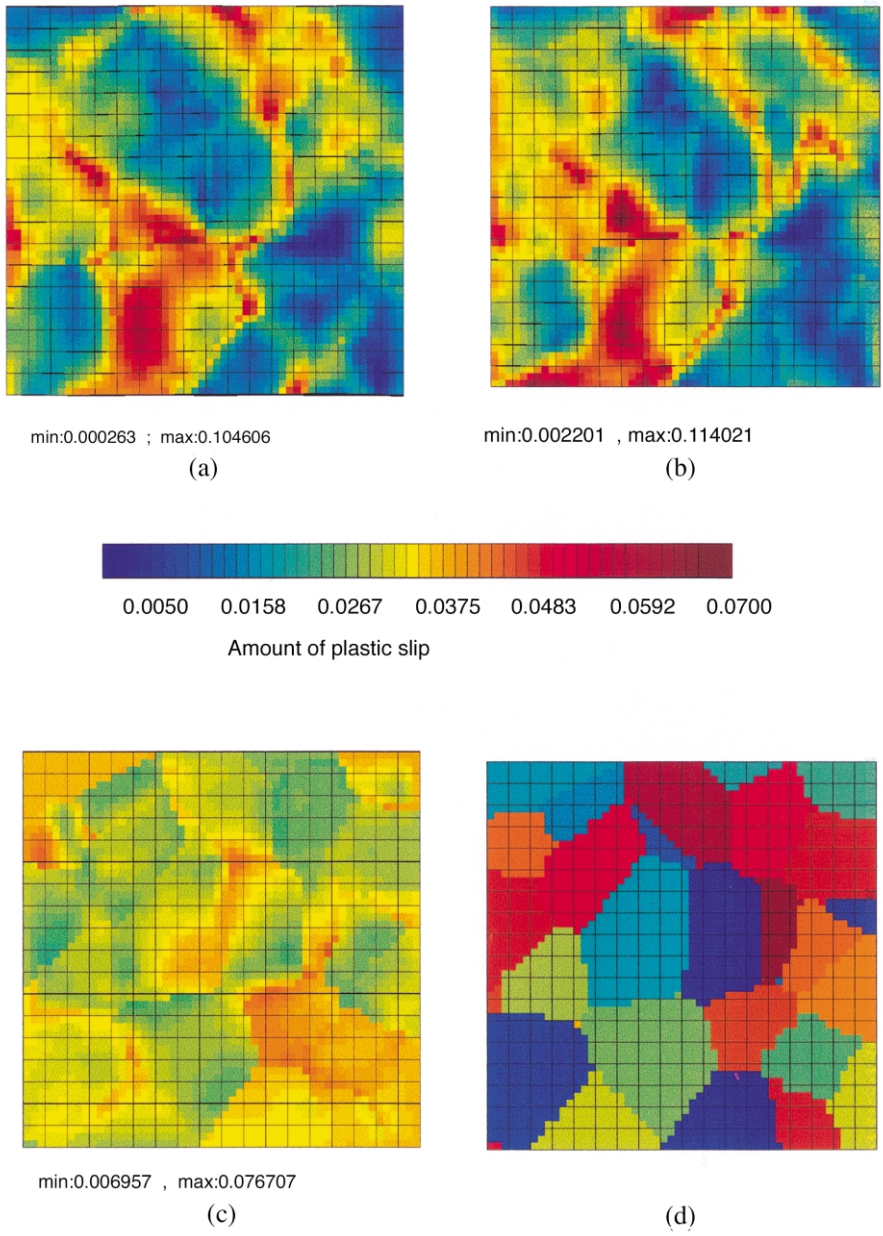

Fig. 12. Contour of the amount of plastic slip on a lateral face of the polycrystal subjected to the conditions: (a) 4FF; (b) MB; (c) HSB; (d) associated grain map.

4.5. Analysis on contour plots

Figs. 12 and 13 illustrate the local effect of a free surface on the external contour of the aggregate. They confirm the effects observed with averaged values: the amount of plastic slip, for instance, reaches larger values in the case 4FF than in the case of HSB. As a natural consequence, the distribution of plastic slip appears more heterogeneous in the case of a free surface. This remark is consistent with the

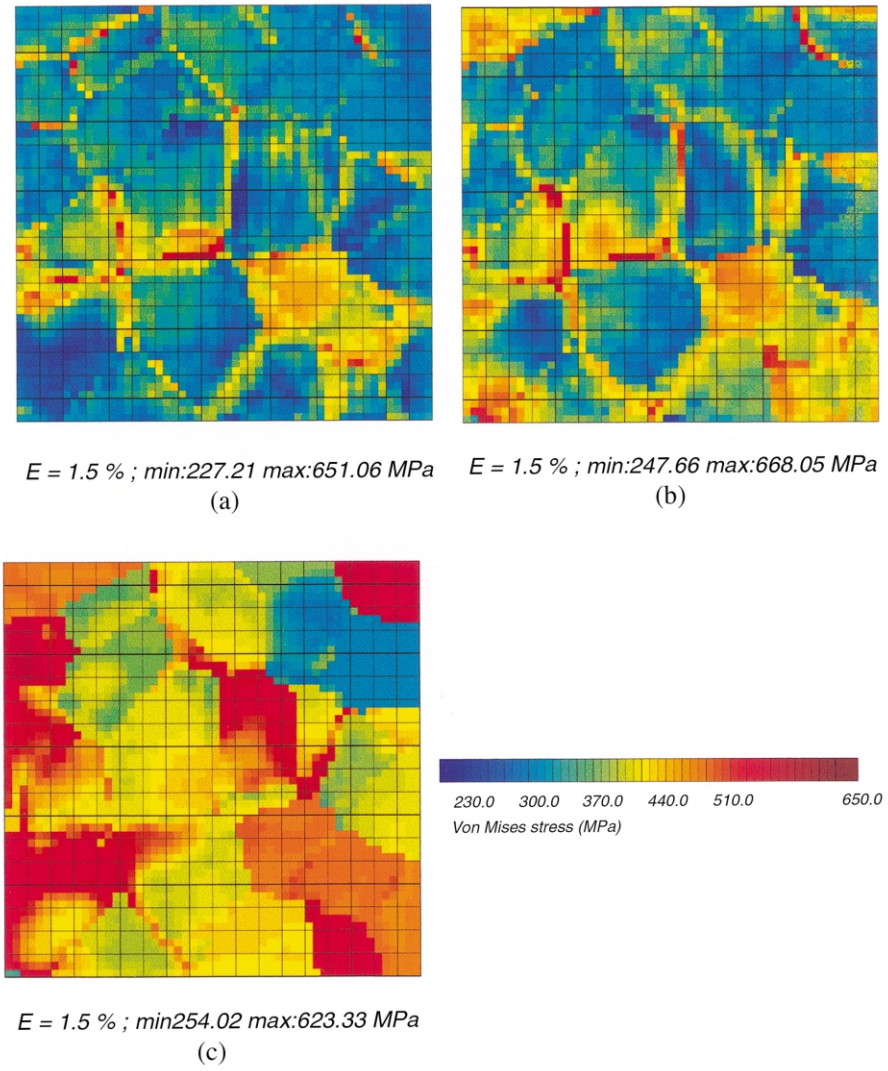

Fig. 13. Contour of the von Mises stress on a lateral face of the polycrystal subjected to the conditions (a) 4FF; (b) MB; (c) HSB; (d) shows the corresponding grain map.

comparison made on the axial stress: larger averaged stress (case HSB) can also be associated with a more heterogeneous field.

Fig. 13 combined with Fig. 12 also provides interesting information about the mechanisms involved in the accommodation of the deformations of the grains at the surface of the cube: as it was found experimentally (Ungár et al., 1998; Zehetbauer et al., 1999) and by simulations (Teodosiu et al., 1991; Harder, 1999), internal stresses appear larger near the grain boundaries than within the grain interiors, more particularly in the cases of mixed boundary conditions. The regions with high stress levels are commonly considered as those where dislocation densities are the highest (Teodosiu et al., 1991). Moreover, according to (Liu et al., 1998), the majority of the dislocations at the grain boundaries are related to active slip systems predicted by a Schmid factor analysis. Consequently, since the resolved shear stress on a slip system is related to the stress in the grain through a Schmid factor, the resulting slip activity provides some qualitative information on the dislocation density. As the amount of plastic slip defines the sum of the slip over the slip systems, a region where the amount of plastic slip is the most pronounced may correspond to a region of high amount of stress, specially if it is close to a grain boundary. This is consistent with the observed contours of the amount of slip (Fig. 12): the regions of high amount of stress are also those of the most developed plastic slip (which is not necessarily true about the equivalent deformation).

Consequently, as the aggregate subjected to HSB proved to produce the highest amount of plastic slip (Fig. 10c) as well as the highest amount of stress, the effect observed can be said to be the effect of a *softened free surface:* in a polycrystalline aggregate with a free surface, the plastic deformations develop more freely. This corresponds to the case when dislocations simply vanish as they reach the surface, instead of dividing into two halves of a dipole, one which leaves the surface, the other which remains thus increasing the dislocation density (Ungár et al., 1998).

5. Conclusion

Finite element computations of a synthetic polycrystal are performed, using large finite element meshes to represent a significant number of grains with a significant number of Gauss points, and crystallographic viscoplastic laws. It has been observed that the mechanical response is successfully captured by a self-consistent approach, at least for the global stress–strain curve, and the averaged values for each phase: the agreement is very good and relatively independent of the applied boundary conditions, so that the presented aggregates are not far from being representative volume elements. We obtain however 6–10% variation on the overall axial stress level. A systematic study on the estimation of the typical size of a RVE for a polycrystalline material is in progress, it may also be related to an intrinsic length scale of the material. In the constitutive modeling of single crystals used in this work, no intrinsic length scale can be introduced, so that no absolute size effect can be accounted for. Moreover, relative size effects regarding the ratio between grain size and the size of the cube play a major role in the definition of a RVE. Current work

focuses on the introduction of generalised plasticity models (Forest, 1998) in order to introduce an absolute scale for the aggregate and describe grain size effects.

On the other hand, the major quantitative result deals with the local heterogeneity, which is not taken into account by the models involving average fields. Variations of $\pm 100\%$ can be found on quantities like the axial stress component averaged in one grain due to the action of the real neighborhood. These variations are still bigger if local stress/strain contours are considered. Inside each grain, dramatic redistributions related to the plastic flow can lead to cumbersome stress states, with local axial compression under global tension load. Surprisingly, plastic deformation structures develop at a larger scale than the grain, showing that self-organisation phenomena related to neighborhood effects play a major role: the areas of intense plastic slip are clearly connected neither with a given crystallographic orientation nor with a given position with regards to surface, but it is the result of the joint effect of several grains.

Collecting data concerning these various intragranular stress/strain states will allow us to revisit damage development in polycrystalline materials. The present work already enables us to characterise the surface effect: by taking the case of homogeneous strain as a reference, it can be shown that for a free surface, the axial stress is lower, and the plastic strain is larger, even if the total amount of plastic slip is lower. Since the constraints are lower at the surface, the plasticity development is freer, and each slip system is more efficient, a lower number of slip systems being active. These results confirm other numerical attempts to characterise the softening in the vicinity of the surface (Pilvin, 1998; Sauzay and Gilormini, 1999). Nevertheless, the effects due to the neighborhood of a grain are more significant than the surface effect. The present paper tries to bring a new element in the discussion by pointing out the well-known fact that the classical models of an inclusion embedded in a homogeneous medium do not capture the intragranular effect, and underestimate the real heterogeneity in the material.

References

Barbe, F., Cailletaud, G., Forest, S., 1999. F.E. study of the surface effect in polycrystalline aggregates. In: Sung Pil Chang (Ed.), Transactions of the 15th international conference on structural mechanics in reactor technology, vol. XII, SMIRT-15. Korean Nuclear Society, Seoul, Korea, pp. 17–28.

Barbe, F., Decker, L., Jeulin, D., Cailletaud, G., 2001. Intergranular and intragranular behavior of polycrystalline aggregate. Part 1: F.E. model. International Journal of Plasticity, 17, 513–536.

Berveiller, M., Zaoui, A., 1979. An extension of the self-consistent scheme to plastically flowing polycrystal. J. Mech. Phys. Solids 26, 325–344.

Forest, S., 1998. Modeling slip, kink and shear banding in classical and generalized single crystal plasticity. Acta Mater. 46 (9), 3265–3281.

Fourie, J.T., 1967. The flow stress gradient between the surface and centre of deformed copper single crystals. Phil. Mag. 15, 735–756.

Harder, J., 1999. A crystallographic model for the study of local deformation processes in polycrystals. International Journal of Plasticity 15 (6), 605–624.

Huet, C., 1990. Application of variational concepts to size effects in elastic heterogeneous bodies. J. Mech. Phys. Solids 38, 813–841.

Liu, Q., Juul Jensen, D., Hansen, N., 1998. Effect of grain interaction on deformation structure in cold-rolled polycrystalline aluminium. Acta Mater. 46 (16), 5819–5838.

Mughrabi, H., 1970. Investigations of plastically deformed copper single crystals in the stress-applied state. Physica Status Solidi 39, 317–327.

Mughrabi, H., 1992. Introduction to the viewpoint set on: surface effect in cyclic deformation and fatigue. Scripta Metal. Mater. 26, 1499–1504.

Nakada, Y., Chalmers, B., 1964. Effects of surface conditions on the stress–strain curves of aluminium and gold single crystals. Trans. Met. Soc. AIME 230, 1339–1344.

Pangborn, R.N., Weissmann, S., Kramer, I.R., 1981. Dislocations distribution and prediction of fatigue damage. Metal. Trans. 12A, 109–120.

Pilvin, P., 1998. Une approche simplifiée pour schématiser l'effet de surface sur le comportement mécanique d'un polycristal. J. de Physique IV 8 (4), 33–38.

Quilici, S., Cailletaud, G., 1999. F.E. simulation of macro-, meso- and micro- scales in polycrystalline plasticity. Comput. Mat. Sci. 16 (1–4), 383–390.

Quilici, S., Forest, S., Cailletaud, G., 1998. On size effects in torsion of multi- and polycrystalline specimens. J. de Physique IV 8 (8), 197–205.

Sauzay, M. and Gilormini, P., 1999. Surface effect, fatigue and microplasticity. In: 4th International Conference on Constitutive Laws in Engineering Materials, Troy, USA.

Teodosiu, C., Raphanel, J.L., Tabourot, L., 1991. Finite element simulation of the large elastoplastic deformation of multicrystals. In: Teodosiu, C., Raphanel, J.L., Sidoroff, F., (Eds.), Proceedings of the International Seminar Mecamat'91: Large Plastic Deformations, Fundamental Aspects and Applications to Metal Forming, Fontainebleau, France, pp. 153–168.

Ungár, T., Langford, J.I., Cernik, R.J., Vörös, G., Pflaumer, R., Oszlányi, G., Kovács, I., 1998 . Microbeam X-ray diffraction study of structural properties of polycrystalline metals by means of synchrotron radiation. Mat. Sci. Engng. A247, 81–87.

Ungar, T., Mughrabi, H., Wilkens, M., 1982. An X-ray line-broadening study of dislocations near the surface and in the bulk of deformed copper single crystals. Acta Metall. 30, 1861–1867.

Zehetbauer, M., Ungár, T., Kral, R., Borbély, A., Schafler, E., Ortner, B., Amenitsch, H., Bernstorff, S. , 1999. Scanning X-ray diffraction peak profile analysis in deformed Cu-polycrystals by synchrotron radiation. Acta Mater. 47 (3), 1053–1061.